Efficient Fabrication of Carbon Nanotube Micro Tip Arrays by Tailoring Cross-Stacked Carbon Nanotube Sheets

ARTICLE *in* NANO LETTERS · MARCH 2012

Impact Factor: 13.59 · DOI: 10.1021/nl300271p · Source: PubMed

6 AUTHORS, INCLUDING:

Yang Wei
Tsinghua University
53 PUBLICATIONS **982** CITATIONS
SEE PROFILE

Peng Liu
King Abdullah University of Science and Techn…
134 PUBLICATIONS **1,534** CITATIONS
SEE PROFILE

Qunqing Li
Tsinghua University
114 PUBLICATIONS **4,398** CITATIONS
SEE PROFILE

NANO LETTERS

Letter

pubs.acs.org/NanoLett

Efficient Fabrication of Carbon Nanotube Micro Tip Arrays by Tailoring Cross-Stacked Carbon Nanotube Sheets

Yang Wei,* Peng Liu, Feng Zhu, Kaili Jiang, Qunqing Li, and Shoushan Fan

Department of Physics and Tsinghua-Foxconn Nanotechnology Research Center, Tsinghua University, Beijing 100084, P. R. China

ABSTRACT: Carbon nanotube (CNT) micro tip arrays with hairpin structures on patterned silicon wafers were efficiently fabricated by tailoring the cross-stacked CNT sheet with laser. A blade-like structure was formed at the laser-cut edges of the CNT sheet. CNT field emitters, pulled out from the end of the hairpin by an adhesive tape, can provide 150 μA intrinsic emission currents with low beam noise. The nice field emission is ascribed to the Joule-heating-induced desorption of the emitter surface by the hairpin structure, the high temperature annealing effect, and the surface morphology. The CNT emitters with hairpin structures will greatly promote the applications of CNTs in vacuum electronic devices and hold the promises to be used as the hot tips for thermochemical nanolithography. More CNT-based structures and devices can be fabricated on a large scale by this versatile method.

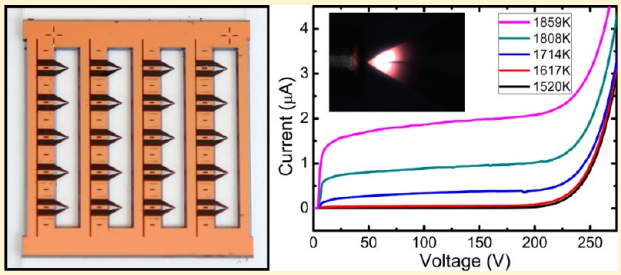

KEYWORDS: *Carbon nanotube, field emission, thermal field emission, hairpin structure*

Carbon nanotubes (CNTs) are promising field emitters for their high aspect ratio, high electrical and thermal conductivity, great mechanical strength, and chemical inertness,[1−4] and CNT field emitters have become attractive candidates for upgrading thermionic electron sources and conventional field emitters.[5−8] Some recent studies have reported that CNT field emitters are sensitive to adsorbents and the ion bombardments,[9,10] similar to conventional electron sources. The solution that has been adopted in commercial products is using hairpin structures,[11−13] where a tungsten wire is bent to V shape, and a tungsten tip, the electron emitter, is assembled at the kink of the hairpin.[14,15] Direct currents are applied through the tungsten wire to heat the tip, and the high temperature induced by joule heating can effectively remove the surface contaminants and smooth the surface roughness. It will be a promising way for CNT cathodes to resolve these problems by elevating the operating temperatures,[16] and it is still a challenge to integrate efficiently CNT field emitters to a heater.

Aligned multiwalled carbon nanotube (MWCNT) films dry spun from superaligned CNT arrays are a special assembly of CNTs, where CNTs are well-aligned and neighboring CNTs are connected to each other by strong van der Waals interactions.[17] The superaligned CNT films have opened up the possibilities of fabricating CNT devices with uniform properties on a large scale, which are currently attracting intense interest in the field of nanoscience and nanotechnology. Novel applications of these transparent freestanding thin films have been developed, such as transparent conductive films, electron sources, transmission electron microscopy (TEM) grids, loudspeakers, touch panels, aerogel muscles, electrodes of Lithium-ion batteries, and so on.[18−23] These aligned CNT films also provide us probabilities to fabricate CNT hairpin structures, which can be used to heat the CNT field emitters.

Here we report an efficient fabrication of hairpin-structured CNT micro tip arrays using MWCNT sheets. Multi layers of free-standing aligned CNT films were cross-stacked together to form a robust CNT sheet, and a piece of CNT sheet was transferred and attached on a patterned silicon wafer. The CNT was then cut into micro tip arrays with hairpin structures by a focused laser beam. A blade-like structure was formed at the laser-cut edges of the CNT sheet. An effective surface treatment was further developed by using adhesive tape to pull CNT tips out from the end of the hairpin. The as-fabricated CNT tips can provide intrinsic field emission currents of ∼150 μA by heating them with the hairpin to remove the surface adsorbents. Raman spectroscpy proved the quality improvement of the CNT tips, which should be attributed to the high temperature annealing. It is possible to upgrade the conventional electron sources with the new CNT hairpin structures.[15,24] The CNT micro tips also hold the promises to be used as hot tips for thermochemical nanolithography.[25−28] More novel structures can be developed by the versatile method, and the integration of CNT sheets and silicon wafers makes it possible to fabricate CNT devices on silicon wafers on a large scale, such as sensors, AFM cantilevers, MEMS, and so on.

Superaligned MWCNT arrays were grown on 4 in. Si wafers by a low-pressure chemical vapor deposition (LPCVD) method. Iron thin film and acetylene were the catalyst and the precursor for CNT growth. The as-synthesized CNTs are

Received: January 21, 2012
Revised: February 24, 2012
Published: March 20, 2012

   dx.doi.org/10.1021/nl300271p | *Nano Lett.* 2012, 12, 2071−2076

~300 μm in height and 6−15 nm in diameter and have 3−10 graphite layers. Detailscan be referred to our previous works.[17,23] Aligned CNT films was coated onto a 72 mm × 72 mm metal frame layer by layer, as schematically illustrated in Figure 1a. After the stacking process, the CNT sheet was

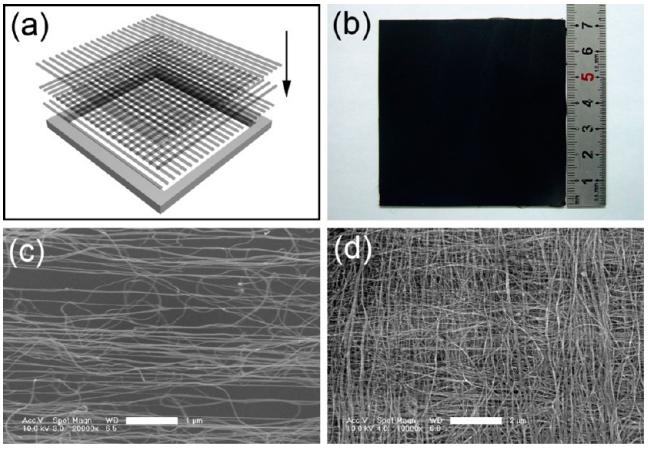

Figure 1. (a) Schematic illustration of the cross-stacked CNT sheet. (b) 72 mm ×72 mm CNT sheet having 50 single layers. (c) SEM image of a single layer of the as-spun aligned CNT film. Scale bar: 1 μm. (d) SEM image of the cross-stacked CNT sheet. Scale bar: 2 μm.

dipped in ethanol solvents and dried in air at room temperature to make CNT firmly compact together. A CNT sheet with 50 single layers is shown in Figure 1b. A scanning electron microscopy (SEM) image of the aligned CNT film drawn from the superaligned CNT array is presented in Figure 1c, where the CNTs are well-aligned and parallel to each other along the drawn direction with a uniform density. Figure 1d is the morphology of the cross-stacked CNT sheet, and the cross structure is illustrated in this panel.

A silicon-nitride-coated silicon wafer was selected as the carrier for the CNT sheets, and it was patterned mainly by photolithography, reactive-ion etching (RIE), and silicon wet etching processes. The silicon nitride film was first etched by a RIE method under the protection of a patterned photoresist layer. The wafer was then dipped into KOH solution, and silicon was etched from the RIE-etched windows in the silicon nitride film. Finally, a layer of 1 μm thick silicon dioxide film was deposited on the wafer by a plasma-enhanced chemical vapor deposition (PECVD) method. The silicon dioxide layer was used as an insulator to cover the naked silicon formed after the wet etching process. Figure 2a shows a patterned 4 in. silicon wafer, which has seven repeating units. The seven units in one wafer were then separated into independent pieces, and Figure 2b shows such an independent unit, 25 mm × 26.8 mm in size. The detailed structure of the V groove is sketched in the inset of Figure 2b. The horizontal short V grooves, as shown in Figure 2b, were used as marks for attaching CNT sheets and wafer cutting. The vertical long V grooves were used to suspend CNT sheet for laser cutting. The CNT micro tip array was arranged to be located on the blank zone in the chip.

A piece of the CNT sheet was then coated on the frame, the insulator-coated silicon. We note that it is difficult to cut off the CNT sheet by a focused laser beam if it is attached on a substrate, as the heat is dissipated through the attached substrate. The CNT sheet was thus prepatterned by laser to avoid this, as shown in Figure 2c. The CNT sheet was attached onto the silicon wafer and aligned with the pattern on wafer by finding the horizontal short V-grooves through the laser-cut windows under an optical microscope. Ethanol solvents were dropped on the surface of the CNT-covered silicon wafer to wet them, and after drying in air at room temperature the CNT

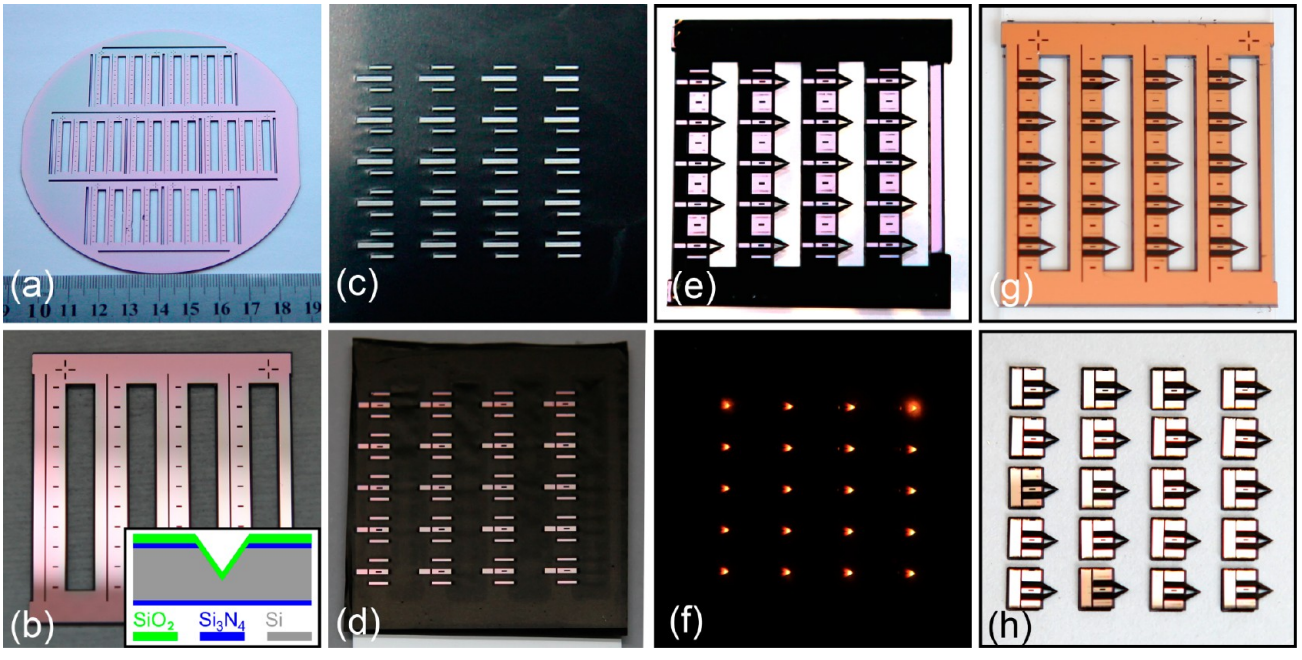

Figure 2. (a) 4 in. patterned silicon wafer having seven repeat units. (b) Independent unit, 25 mm × 26.8 mm in size. The inset sketches the cross section of the V groove. (c) Piece of prepatterned CNT sheet. (d) CNT-coated silicon wafer with their patterns being aligned with each other. (e) 5 × 4 CNT micro tip arrays with hairpin structures. The tips in one row are connected in series, and the four rows are connected in parallel. (f) Corresponding lit CNT micro tip array. (g) 5 × 4 array without interconnections. (h) Independent CNT micro tips; one chip size is 3 mm ×4 mm.

dx.doi.org/10.1021/nl300271p | *Nano Lett.* 2012, 12, 2071−2076

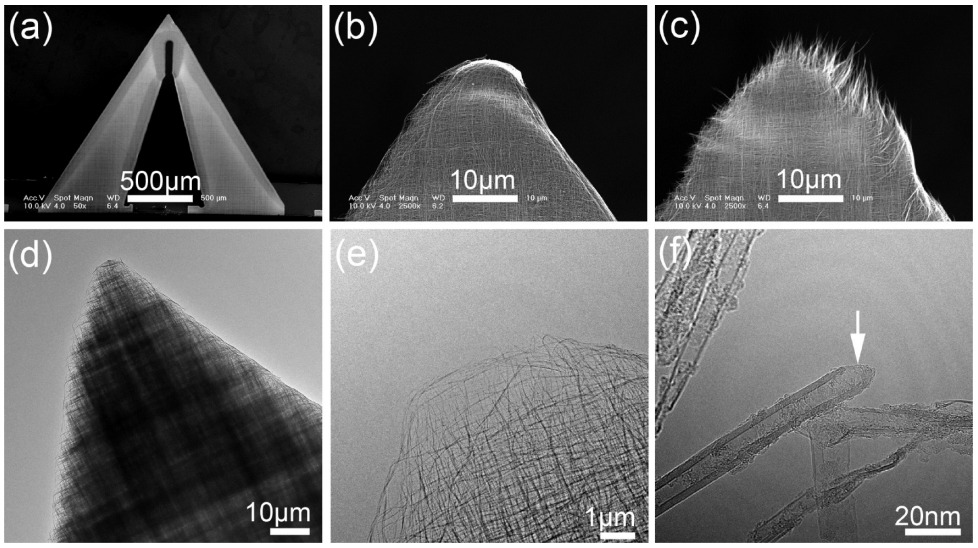

Figure 3. (a) Panoramic view of the hairpin CNT micro tip. The hairpin angle is 60°. The two arms become narrowing to the tip. (b) Tip is zoomed in in this panel. The laser-cut edge is regular. (c) Tip morphology with adhesive tape treatment. Individual CNT tips can be found at the end. (d,e) TEM images of the micro tip reveal the blade-like structure at the edge. (f) MWCNT with open end marked by an arrow. Amorphous matter can also be found on the tubes.

sheet was coated on the silicon substrate firmly, as shown in Figure 2d.

A beam of YAG laser was introduced to cut the CNT sheet into 5 × 4 CNT micro tip arrays with hairpin structures. The wavelength of the laser is 1.06 μm, and the FWHM of the focus is 30 μm. The power output and the scanning speed of the laser beam were set as 3.6 W and 100 mm/S, respectively. The CNT sheet irradiated by the focused laser was burnt quickly in air and was thus cut into the designed figures. The as-fabricated CNT microtip array is shown in Figure 2e, and the hairpin angle is 60°. The five tips in one row are still connected in series by remaining CNTs, and the four rows are connected in parallel. With this arrangement, the tip array was uniformly heated to the incandescent state by direct currents, as illustrated in Figure 2f. This tells that the as-developed processes have good repeatability. The CNTs connecting the hairpins were cut off by laser along the predesigned V grooves and removed by hand, and the 5 × 4 CNT micro tip array without interconnections is shown in Figure 2g. To study field-emission properties of an individual tip, the array was eventually cut into independent hairpin CNT tips along the V grooves between neighboring CNT tips. The as-fabricated 20 CNT micro tips are presented in Figure 2h, and the size of the small silicon chip is 3 mm × 4 mm.

The tip structures were further studied by SEM and TEM in detail. A full view of one hairpin CNT micro tip is shown in Figure 3a. The hairpin angle is 60°. The two arms become narrow and merge at the tip. To make sure the tip can be effectively heated, the tip width was further decreased by an additional groove also formed by laser writing. The tip width is ~210 μm, defined from the tip end to the top of the groove. The tip morphology with higher magnification is shown in Figure 3b. The tip has an orderly margin, and it is difficult to find any CNT tips at the tip ends. This is not favorable for field emission. A surface-treatment process was further developed by using an adhesive tape to approach and touch the tip end.[29] The CNTs were assembled into tips at the end of the hairpin after the adhesive tape was removed. The tip abundant structures are presented in Figure 3c, and the field emission will benefit from this novel morphologies. The blade-like structure, as shown in Figure 3a, is another attractive feature. The edge of the laser-cut pattern is much thinner than the body part. This is also demonstrated by the TEM observations, as shown in Figure 3d. The bright edge shows that the electron transmittance at the edge is higher, and the edge has a thinner thickness. Figure 3e is a TEM image at the tip end of the CNT hairpin, further revealing that CNTs are sparsely distributed at the margin. TEM observations show that open ends are commonly seen at the laser-cut edges, and Figure 3f presents a MWCNT with open end marked by an arrow. Amorphous matters can also be found on the walls of the tubes. The blade-like edge and the open-ended CNTs should be attributed to the local burning effect induced by the focused laser.

The Joule heating properties of the hairpin CNT structures were studied by feeding direct currents through them. The silicon wafer carrier with an insulating layer made these measurements maneuverable. Two copper fossils were pressed on the two CNT branches, respectively, and direct currents were applied through the hairpin structures with the cooper fossil electrodes. The local heating effect at the CNT hairpin tip is illustrated in Figure 4, and this can be attributed to the gradual-changing width and the detailed structure at the tip. The four panels of Figure 4 present the hot CNT micro tip at 1261, 1420, 1520, and 1714 K, respectively. The temperatures of the hot tips were determined by fitting the incandescent light spectrum with the blackbody radiation law.[20,24] The current−voltage (IV) characteristic of the CNT hairpin is shown in Figure 5a. The slopes change with the heating voltage, and this is caused by the temperature-dependent resistance of the CNTs.[20] The temperature dependences on heating voltage and power are illustrated in Figure 5b,c, respectively. The tip can be heated to 1860 K by a 13.5 V heating voltage and a 586 mW heating power.

Field-emission properties were studied under a 2 × 10^{-5} Pa dynamic vacuum. A CNT micro tip with hairpin structure carried by the silicon chip was assembled to a 3D manipulator. By using the manipulator, the tip was pointed at the center of a polished cross section of a nickel rod with a 100 μm gap

dx.doi.org/10.1021/nl300271p | Nano Lett. 2012, 12, 2071−2076

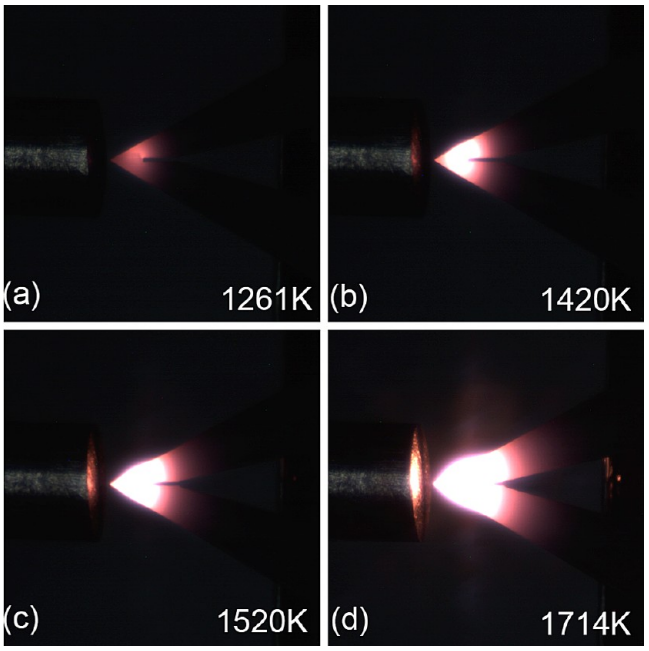

Figure 4. Hot CNT micro tip at 1261, 1420, 1520, and 1714 K, respectively. These optical microscope observations tell that the tip structure design can effectively achieve hot tips at the end of the hairpin structures.

between them. The diameter of the nickel rod was 1 mm, and the testing configuration is also shown in Figure 4. Field-emission properties were measured by applying positive voltages on the nickel anode with a Keithley 2410 sourcemeter. Figure 5d comparatively presents the field-emission IV curves of the CNT micro tips at room temperature and 958 K. The CNT micro tips can provide emission currents of about 150 μA. The two IV curves tell that field-emission currents were decreased by Joule heating, and the noise was significantly decreased as the IV curve became smooth. These are further clarified by Figure 5f, which shows that the emission current changes as the temperature switches between RT and 958 K. Both the FE currents and the noise decrease after being heated and recover after stopping heating. These phenomena are attributed to Joule-heating-induced desorption of the adsorbents on the CNT field emitters, and water is believed to be the dominant species that influences the FE of MWCNTs on the basis of previous theoretical calculations.[9] The movement of the adsorbents at RT can also induce significant noise.[15]

The inset of Figure 5d is the corresponding Fowler–Nordheim (FN) plots. The FN curve becomes a perfect straight line after the CNT microemitters are heated. The smooth and straight FN curve shows that the CNT field emitters can provide intrinsic field emission currents, which agree well with the conventional FN theory by removing the adsorbents on the emitters.[9,30−32] The field enhancement factor of the CNT micro tip emitter is 2091, which is deduced from the slope of the FN curve by setting the work function as 4.6 eV.[20,24] Three main factors contribute to the field-enhancement factor. The first is that the radius of curvature is 5 μm at the tip end, which can be measured from Figure 3e; second, the thickness at the edge is nanoscaled because it tends to be single-layered, as shown in Figure 3e; the third is the tip abundant morphology at the tip end induced by the surface treatment process.[33]

Thermal field electron emission was also observed. By increasing the cathode temperatures, we found that the anode can connect thermionic electron currents when the voltage was still lower than the threshold voltage of field emission during the field-emission IV measurements. The IV curves at different temperatures are presented in Figure 5e, and temperature-dependent thermal field emission is shown in the inset. The thermal field emission becomes significant when the temperature is over 1700 K. The thermal field emission is attributed to both the high temperature at the CNT tips and their large field enhancement factor.[34] High temperature cannot only evaporate electrons from the CNTs but also improve the degree of graphitization. After these thermal field-emission measurements, the tip was further analyzed by Raman spectroscopy using a 514 nm laser excitation, and the results are illustrated in Figure 6. Effective removal of the structural defects is supported

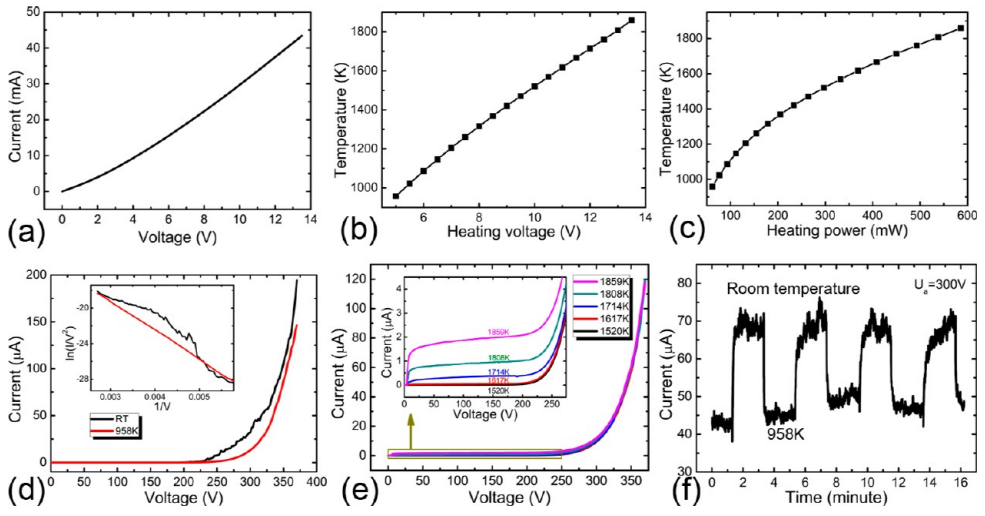

Figure 5. (a) IV curve of the CNT hairpin. (b,c) Heating voltage and heating power-dependent temperatures of the as-fabricated CNT micro tips. (d) Comparative field emission IV curves of the CNT micro tip with and without Joule heating. Inset is the corresponding FN curves. (e) Field-emission IV curves of the CNT micro tip at different temperatures. Thermal field emission can be seen in the inset. (f) Emission current change due to the temperature switching. Both the FE currents and the noise decrease after being heated and recover after stopping heating.

dx.doi.org/10.1021/nl300271p | *Nano Lett.* 2012, 12, 2071−2076

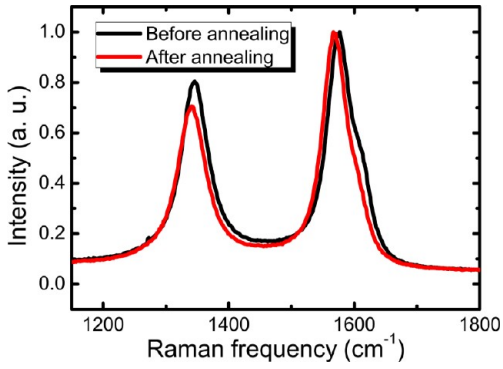

Figure 6. Raman spectra of the MWCNT tip before and after high temperature annealing (black and red solid lines).

by both the low-intensity D-band (defect mode) at 1350 cm^{-1} and the peak downshift, which is ascribed to the high-temperature annealing effects.[21,35]

The method is an efficient technology to fabricate CNT micro tips with the hairpin structures. Mass production of such CNT micro tips can be achieved by scale up of the substrates and the CNT sheets, as this work is based only on a 25 mm × 26.8 mm patterned silicon substrate and a piece of a CNT sheet with the same size. CNT sheets larger than 4 in. can be fabricated because we have realized synthesizing superaligned CNT arrays on 8 in. silicon wafers.[36] Improvement of the integration level is another promising direction, as the period on the chip is only 6 mm × 4 mm. Furthermore, the technology we developed is a versatile method, and we fabricated more structures by tailoring the multilayered cross-stacked CNT sheets with a focused laser beam. Figure 7a presents a CNT

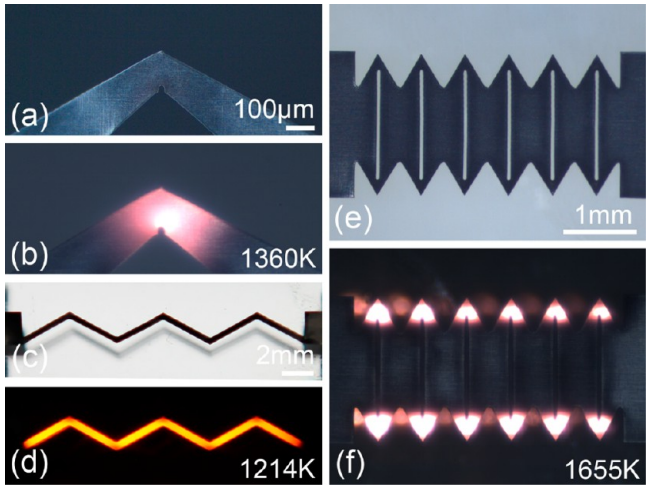

Figure 7. (a,b) CNT micro tip with 120° hairpin angle without and with electrical heating. (c,d) Zig-zag-shaped CNT structure without and with electrical heating. (e,f) Symmetrical multitipped structures with hairpin structures without and with electrical heating.

structure with 120° hairpin angle, and the corresponding hot tip induced by Joule heating is shown in Figure 7b. Figure 7c,d shows a zigzag structure with and without electrical heating, and it was fabricated also by tailoring CNT sheets with laser. Figure 7e shows a more complicated pattern, where symmetrical CNT tips with hairpin structures are connected in series. All of the tips were locally heated to incandescent state, and they are shown in Figure 7f. From these experiments, it is found that tailoring CNT sheets is a general method to fabricate various CNT patterns.

The CNT micro tips we developed are nice electron emitters. It is promising to assemble them into vacuum electronic devices as electron sources, such as SEM, TEM,[37] electron momentum spectroscopy instrument,[24] X-ray tubes,[38] saddle gauges,[39] and so on. The CNT micro tips have high compatibility with the conventional vacuum electronic devices, as they inherit the merits of the conventional hairpin structured electron sources. It should be noted that the CNT-based hairpins have some new characters. CNT field emitters can effectively lower the driving voltages because CNTs have high field enhancement factors. Localized high temperature, which is different to conventional hairpin emitters, makes the CNT micro tips have lower power consumption. The ultralow heat capacity per unit area (HCPUA) of the CNT sheets will remarkably shorten the time needed to stabilize the cathodes.[40] The emitters made up of CNT sheets are flexible, and this can greatly expand the application of CNT emitters. The basic structure characteristics of the novel CNT tip, including nanoscaled thickness and the localized high temperatures, decide that the hot tip is a possible candidate for thermochemical nanolithography, which recently received much research attention.[25−28] Successfully integrating CNT sheets into silicon wafer is another important progress achieved in this work because it is an ideal combination of CNT technology and conventional silicon wafer processes. More CNT-based devices will possibly benefit from the technology we developed, such as sensors, AFM cantilevers, MEMS, and so on.

In summary, we proposed a novel CNT-based hairpin structure, and CNT micro tip arrays with hairpin structure were successfully fabricated on a patterned silicon wafer by tailoring cross-stacked CNT sheets with a focused laser beam. By using an adhesive tape to modify the hairpin tip, CNT field emitters were perfectly integrated to the hairpin-structured CNT heater. The CNT tips were locally heated by direct currents to effectively remove adsorbents on the CNT emitters, and the emitters thus provided intrinsic field emission currents of 150 μA with low noise. Raman spectroscopy studies further revealed that the high local temperature annealing can improve the quality of the CNTs at the tips. The ideal integration of CNTs and the widely used hairpin structures will greatly promote the applications of CNT field emitters in the field of vacuum electronic devices, and they will hold the promises to be used as the hot tips for thermochemical nanolithography. The technology is a versatile method because various structures were fabricated by using the robust flexible CNT sheets. The integration of CNT sheets and silicon wafer is also noticeable, and the combination makes it possible to fabricate many CNT-based devices on silicon wafers with large scale, such as sensors, AFM cantilevers, MEMS, and so on.

AUTHOR INFORMATION

Corresponding Author

*E-mail: WeiYang@tsinghua.edu.cn.

Notes

The authors declare no competing financial interest.

■ ACKNOWLEDGMENTS

We acknowledge the financial support from the National Basic Research Program of China (2012CB932301) and the NSFC (51102147, 51102144, 90921012).

■ REFERENCES

(1) Iijima, S. *Nature* **1991**, *354*, 56−58.
(2) Fan, S. S.; Chapline, M. G.; Franklin, N. R.; Tombler, T. W.; Cassell, A. M.; Dai, H. J. *Science* **1999**, *283*, 512−514.
(3) Lan, Y. C.; Wang, Y.; Ren, Z. F. *Adv. Phys.* **2011**, *60*, 553−678.
(4) Baughman, R. H.; Zakhidov, A. A.; de Heer, W. A. *Science* **2002**, *297*, 787−792.
(5) Deheer, W. A.; Chatelain, A.; Ugarte, D. *Science* **1995**, *270*, 1179−1180.
(6) Saito, Y.; Hamaguchi, K.; Uemura, S.; Uchida, K.; Tasaka, Y.; Ikazaki, F.; Yumura, M.; Kasuya, A.; Nishina, Y. *Appl. Phys. A: Mater. Sci. Process.* **1998**, *67*, 95−100.
(7) Saito, Y.; Uemura, S. *Carbon* **2000**, *38*, 169−182.
(8) Bonard, J. M.; Kind, H.; Stockli, T.; Nilsson, L. A. *Solid-State Electron.* **2001**, *45*, 893−914.
(9) Maiti, A.; Andzelm, J.; Tanpipat, N.; von Allmen, P. *Phys. Rev. Lett.* **2001**, 87.
(10) Bormashov, V. S.; Baturin, A. S.; Nikolskiy, K. N.; Tchesov, R. G.; Sheshin, E. P. *Surf. Interface Anal.* **2007**, *39*, 155−158.
(11) Kamigaito, O. *Jpn. J. Appl. Phys.* **1965**, *4*, 604−612.
(12) Murray, R. G.; Collier, R. J. *Rev. Sci. Instrum.* **1977**, *48*, 870−873.
(13) Winkler, O. *Optik* **1988**, *78*, 111−116.
(14) Dyke, W. P.; Charbonnier, F. M.; Strayer, R. W.; Floyd, R. L.; Barbour, J. P.; Trolan, J. K. *J. Appl. Phys.* **1960**, *31*, 790−805.
(15) Swanson, L. W.; Martin, N. A. *J. Appl. Phys.* **1975**, *46*, 2029−2030.
(16) Liu, P.; Jiang, K. L.; Wei, Y.; Liu, K.; Liu, L. A.; Fan, S. S. *J. Vac. Sci. Technol., B* **2010**, *28*, 736−739.
(17) Jiang, K. L.; Li, Q. Q.; Fan, S. S. *Nature* **2002**, *419*, 801−801.
(18) Zhang, M.; Atkinson, K. R.; Baughman, R. H. *Science* **2004**, *306*, 1358−1361.
(19) Zhang, M.; Fang, S. L.; Zakhidov, A. A.; Lee, S. B.; Aliev, A. E.; Williams, C. D.; Atkinson, K. R.; Baughman, R. H. *Science* **2005**, *309*, 1215−1219.
(20) Wei, Y.; Jiang, K. L.; Feng, X. F.; Liu, P.; Liu, L.; Fan, S. S. *Phys. Rev. B* **2007**, 76.
(21) Wei, Y.; Jiang, K. L.; Liu, L.; Chen, Z.; Fan, S. S. *Nano Lett.* **2007**, *7*, 3792−3797.
(22) Aliev, A. E.; Oh, J. Y.; Kozlov, M. E.; Kuznetsov, A. A.; Fang, S. L.; Fonseca, A. F.; Ovalle, R.; Lima, M. D.; Haque, M. H.; Gartstein, Y. N.; Zhang, M.; Zakhidov, A. A.; Baughman, R. H. *Science* **2009**, *323*, 1575−1578.
(23) Jiang, K. L.; Wang, J. P.; Li, Q. Q.; Liu, L. A.; Liu, C. H.; Fan, S. S. *Adv. Mater.* **2011**, *23*, 1154−1161.
(24) Liu, P.; Wei, Y.; Jiang, K. L.; Sun, Q.; Zhang, X. B.; Fan, S. S.; Zhang, S. F.; Ning, C. G.; Deng, J. K. *Phys. Rev. B* **2006**, 73.
(25) Popescu, A.; Woods, L. M. *Appl. Phys. Lett.* **2009**, 95.
(26) Kim, S.; Bastani, Y.; Lu, H. D.; King, W. P.; Marder, S.; Sandhage, K. H.; Gruverman, A.; Riedo, E.; Bassiri-Gharb, N. *Adv. Mater.* **2011**, *23*, 3786−3790.
(27) Szoszkiewicz, R.; Okada, T.; Jones, S. C.; Li, T. D.; King, W. P.; Marder, S. R.; Riedo, E. *Nano Lett.* **2007**, *7*, 1064−1069.
(28) Fenwick, O.; Bozec, L.; Credgington, D.; Hammiche, A.; Lazzerini, G. M.; Silberberg, Y. R.; Cacialli, F. *Nat. Nanotechnol.* **2009**, *4*, 664−668.
(29) Vink, T. J.; Gillies, M.; Kriege, J. C.; van de Laar, H. *Appl. Phys. Lett.* **2003**, *83*, 3552−3554.
(30) Luo, J.; Zhang, Z. X.; Peng, L. M.; Xue, Z. Q.; Wu, J. L. *J. Phys. D: Appl. Phys.* **2003**, *36*, 3034−3038.
(31) Grujicic, M.; Cao, G.; Gersten, B. *Appl. Surf. Sci.* **2003**, *206*, 167−177.
(32) Qiao, L.; Zheng, W. T.; Bwen, Q.; Jiang, Q. *Nanotechnology* **2007**, 18.
(33) Nilsson, L.; Groening, O.; Emmenegger, C.; Kuettel, O.; Schaller, E.; Schlapbach, L.; Kind, H.; Bonard, J. M.; Kern, K. *Appl. Phys. Lett.* **2000**, *76*, 2071−2073.
(34) Tuggle, D. W.; Swanson, L. W. *J. Vac. Sci. Technol., B* **1985**, *3*, 220−223.
(35) Behler, K.; Osswald, S.; Ye, H.; Dimovski, S.; Gogotsi, Y. *J. Nanopart. Res.* **2006**, *8*, 615−625.
(36) Feng, C.; Liu, K.; Wu, J. S.; Liu, L.; Cheng, J. S.; Zhang, Y. Y.; Sun, Y. H.; Li, Q. Q.; Fan, S. S.; Jiang, K. L. *Adv. Funct. Mater.* **2010**, *20*, 885−891.
(37) de Jonge, N.; Lamy, Y.; Schoots, K.; Oosterkamp, T. H. *Nature* **2002**, *420*, 393−395.
(38) Sugie, H.; Tanemura, M.; Filip, V.; Iwata, K.; Takahashi, K.; Okuyama, F. *Appl. Phys. Lett.* **2001**, *78*, 2578−2580.
(39) Sheng, L. M.; Liu, P.; Wei, Y.; Liu, L.; Qi, J.; Fan, S. S. *Diam. Relat. Mater.* **2005**, *14*, 1695−1699.
(40) Liu, P.; Liu, L.; Wei, Y.; Liu, K.; Chen, Z.; Jiang, K. L.; Li, Q. Q.; Fan, S. S. *Adv. Mater.* **2009**, *21*, 3563.